Vibration of Bundled Conductors Following Ice Shedding

László E. Kollár, and Masoud Farzaneh, *Fellow, IEEE*
Industrial Chair on Atmospheric Icing of Power Network Equipment (CIGELE) and Canada Research Chair on Engineering of Power Network Atmospheric Icing (INGIVRE) at Université du Québec à Chicoutimi, Québec, Canada, G7H 2B1 (http://www.cigele.ca)

Abstract—**The dynamic behavior of bundled conductors following ice shedding from one subconductor is examined numerically using the finite element method. An existing model of ice shedding from a single conductor is improved by developing a model of spacers which connect subconductors in the span. The resulting system makes it possible to simulate vibrations following ice shedding from one span of an overhead transmission line with twin, triple or quad bundles. Vibration characteristics are evaluated as the following parameters are varied: thickness of shed ice, distance between adjacent spacers and number of subconductors in the bundle. Simulation results will provide information on how the amplitude of vibration and the transient dynamic forces change with the application of spacers. The maximum jump height of the ice-shedding cable, the maximum drop of the loaded cable, and the maximum cable tension are approximated as power functions of ice thickness and the distance between adjacent spacers.**

***Index Terms*—bundle conductors, finite element methods, modeling, ice, load shedding.**

I. Introduction

OVERHEAD transmission lines are exposed to different types of loads, some of which may lead to severe damages. A serious and frequently arising problem in cold climate regions is the ice accreted on cables and on other line elements. Ice accumulation is akin to a heavy static load, whereas ice shedding from cables results in high-amplitude free vibrations and excessive transient dynamic forces. High-amplitude vibrations may cause flashover between adjacent cables, while excessive forces applied at the suspension contacts may break the insulators or, in extreme cases, damage the towers. Therefore, it is important to predict the maximum cable displacement and the maximum cable tension arising during vibrations following ice shedding.

Great efforts have been made to date in order to attenuate high-amplitude cable vibrations and, thereby, protect the transmission lines, since such vibrations are peculiar not only to cold regions but to windy areas as well. A widely used protection method is the application of spacer dampers, which help to maintain the distance between the bundled subconductors and reduce the amplitude of aeolian vibrations and sub-span oscillations. A numerical approach has been applied successfully in recent developments to study vibrations induced by wind, ice shedding or conductor breakage: the finite element method. In one of the first studies on ice shedding, a series of load-dropping tests simulating ice shedding were performed on a five-span section and the maximum jump height of the cable was measured [1]. In a later study, numerical and experimental investigations were carried out on the vibration of a two-span section of a transmission line with a single cable as a result of ice shedding [2]. Reference [3] examined the dynamic response of a similar two-span section after ice sheds from one span, varying several characteristics of the span. Their model was also used to simulate a tower failure which occurred in a 220 kV transmission line following ice shedding [4]. The vibration of a two-span section due to ice shedding from one span was investigated in [5] by considering different types of ice. Reference [6] proposed a model to simulate the mitigation of ice failure and ice shedding in a one-span section due to pulse-type excitation. These models were all elaborated using a commercial finite element analysis software, ADINA [7].

Extensive research has already been done on galloping of bundled conductors, and on ice-shedding-induced vibration of a single cable. The objective of the present study is to develop a spacer model, and analyze the dynamics of bundled conductors following ice shedding from one subconductor, with a special emphasis on how the amount of ice, the distance between adjacent spacers, and the number of subconductors influence the severity of the vibration. After a brief summary on bundle conductor spacers, a finite element model for bundled conductors will be constructed using ADINA. This will be followed by a parametric study where the above mentioned parameters are varied, and power-function approximations are provided to predict the maximum jump height, the maximum drop, and the maximum cable tension.

II. Bundled Conductors with Spacers

Bundled conductors are frequently used for overhead transmission lines where the individual conductors are connected by spacers. The particular construction of each spacer varies depending on the manufacturer, but all of them are designed so as to maintain a constant distance between the subconductors. Though the application of spacers was for electrical reasons, originally, spacers also play an important

L. E. Kollár and M. Farzaneh are respectively member and chairholder of the NSERC/Hydro-Quebec/UQAC Industrial Chair and Canada Research Chair (CRC) on Atmospheric Icing of Power Network Equipment (CIGELE), University of Quebec in Chicoutimi, 555 boulevard de l'Université, Quebec, Canada, G7H 2B1 (e-mail: laszlo_kollar@uqac.ca and farzaneh@uqac.ca).

role from the mechanical point of view, since they help to reduce the severity of cable vibration induced by wind or ice shedding. A spacer of typical design consists of a rigid central frame to which arms are attached via flexible joints. Each of these arms grips one of the subconductors by means of a clamp located at the free end of the arm. The geometrical and physical parameters of some spacers used in bundles of four conductors are provided in [8] where the authors also present a test program aimed to compare the performance of different spacers. Reference [9] summarizes design requirements of spacers including basic engineering requirements, general design parameters, and physical requirements. A recent survey on spacers including types, materials, design characteristics, test methods and field experience is presented in [10]. Illustrations about typical spacers which are used in twin, triple and quad bundles are shown in Fig. 1.

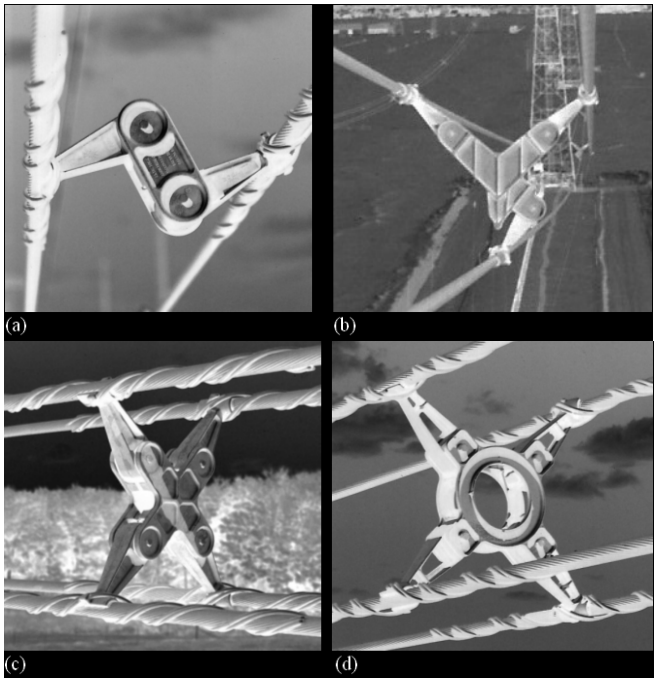

Fig. 1. Spacers in transmission lines (a) twin bundle, (b) triple bundle, (c) and (d) quad bundle

Spacers are subject to various types of loads due to mechanical tensions in the cables, short circuits or high-amplitude vibrations. The highest cable tension and stress during cable vibration usually develop near the suspension clamps as well as in the neighborhood of the spacer clamps. References [11], [12] determined the forces acting at the spacer clamp and developed a mathematical model for vortex-induced vibrations in bundled conductors with spacer dampers. The severity of wake-induced oscillations of bundled conductors was examined on a full-scale experimental line in [13]. In the present study, a finite element model of spacers is constructed and is integrated to the model of one span of an overhead transmission line with bundled conductors as discussed in the subsequent section. This model makes it possible to calculate the forces acting at any part of the conductors including the vicinity of the spacer during the vibration induced by ice shedding from one subconductor.

III. Finite Element Model of a Single Span of Transmission Lines

The finite element model of a single span of bundled conductors with ice load is constructed using ADINA [7]. The cable model and ice model are based on the ones developed in [2] and [3], and will be described below together with the spacer model.

A. Cable Modeling

Two-node isoparametric truss elements with large kinematics are used for cable modeling. A constant initial pre-strain corresponding to the installation conditions is prescribed as an initial condition for all cable elements. This initial strain is obtained from the following formula:

$$\varepsilon_0 = \frac{T_0}{AE} \tag{1}$$

where A is the cross-section of the cable, E is the Young's modulus, and T_0 may be determined from the equilibrium of the cable under its own weight [14]. Cable material properties are defined for tension only, not allowing compression and assuming Hookean small strain behaviour in tension. The cable is assumed to be perfectly flexible in bending and torsion. The mesh selected for the cable contains 100 truss elements in each cable which was found to be adequate for the span length considered in the model (200 m).

Cable damping is considered in the model by defining nonlinear spring elements. The damping force is given in the form $\left|F_D\right| = C\left|\dot{U}\right|^N$, where $\dot{U}$ is the relative velocity between the element end nodes [7]. The structural damping of the cable is modelled by applying viscous dashpot elements in parallel with each cable element with exponent N = 1 and viscous damping constant:

$$C_S = 2\xi\sqrt{AEm} \tag{2}$$

The ξ is the damping ratio, m is the mass per unit length of the cable or the cable-ice composition, and the subscript S refers to structural damping. The damping ratio is chosen as 2% for the bare cable and 10% for the iced cable following the recommendation in [3]. Aerodynamic damping is considered by defining dashpot elements between each cable-element node and the ground, and applying them to the vertical motion of the cable. The exponent N is equal to 2 in this case, while the damping constant is calculated as follows

$$C_A = \frac{1}{2} C_D \rho A_P \tag{3}$$

where C_D is the drag coefficient, ρ is the air density, A_P is the projected area, and the subscript A refers to aerodynamic damping. The drag coefficient, C_D, is assumed to be 1.25, as proposed in [15].

B. Modeling Ice Load and Ice Shedding

Ice load is taken care of by assuming that cable element

density in the static analysis increases proportionally with the weight of ice load. This configuration defines the static equilibrium of the ice-loaded cables. In order to simulate ice shedding, density of the subconductor where ice sheds from is decreased in the dynamic analysis [3]. Thus, the density of an ice-shedding cable is different in the static than in the dynamic case, which causes an abrupt change in the mass matrix and leads to vibrations. The dynamic analysis is carried out to simulate transient vibrations only. In order to obtain the final steady state, it was found more effective to perform an additional static analysis. Since ice failure due to the resulting vibrations is not considered, ice sheds from one subconductor only, while the other subconductors always bear the same amount of ice.

The density of ice depends on the type of ice that accumulates on the cable. The types of ice or snow that may accrete on cables are rime ice, glaze ice, frost, dry snow and wet snow. In general, wet snow, rime ice and glaze ice appear most often on transmission lines, and glaze ice causes the highest ice load. Since investigating the effects of ice type is out of the scope of the present study, the model considers glaze ice accretion which is assumed to have a constant density of 900 kg/m^3.

C. Spacer Modeling

A spacer model was already presented in our former study [16], where spacers were modeled by two-dimensional beam elements. This approach is improved here by considering the flexibility and damping properties of the spacer. Two-node truss elements associated with nonlinear elastic material are applied in order to achieve this goal. The calculation of mass, damping, stiffness matrices and load vector, as well as the construction of the equations of motion for truss elements are discussed briefly in [16], and in detail in [17]. A cubic stress-strain curve describes the material of spacer arms which are allowed to rotate a few degrees around the joint with increasing resistance until the rotation is blocked. Further deformation may occur only by the elongation of the material, which is modeled by a linear stress-strain curve. Thus, the force – deformation relationship, $F_s(\Delta l)$, which describes the flexibility of the spacer, is given by the following formula:

$$F_s = \begin{cases} c_{s3}\Delta l^3 & \text{if} \quad \Delta l < |\Delta l_{cr}| \\ c_{s0} + c_{s1}\Delta l & \text{if} \quad \Delta l \geq |\Delta l_{cr}| \end{cases} \tag{4}$$

where Δl_{cr} is the increase of spacer length at the maximum angle of arm rotation. The constants, c_{s0}, c_{s1} and c_{s3} are obtained from the conditions that the tangent of the force – deformation relationship at the connection, Δl_{cr}, should be equal to $E_s A_s / l_s$, and that the cubic and linear functions take the same value at the connection. The parameters, E_s, A_s and l_s are the Young's modulus, cross section and length of spacer, respectively. The stress-strain relationship may readily be deduced from (4).

Spacers for a twin bundle are simple rods clamped to a conductor at each end. The geometry of spacers for triple and quad bundles is shown in Fig. 2. The envelope dimension of spacers is determined by the distance between two subconductors, which is 0.5 m. Spacers for a triple and for a quad bundle consist of 6 and 8 truss elements, respectively. Dimensions are chosen so that mass and inertia are in a realistic range in accordance with the spacers examined in [8]. The elements modeling the frame have linear elastic material properties, and a cross section of 8 cm in height and 4 cm in width. The elements applied for the arms are associated with the nonlinear elastic material described in the previous paragraph, and they have a cross section of 6 cm in height and 2 cm in width. The material properties are defined to be similar to those of aluminum (density of 2700 kg/m^3, Young's modulus of 70 GPa and Poisson's ratio of 0.35).

The damping properties of spacers are modeled by nonlinear spring elements with N = 1, and the damping constant may be obtained from (2) after substituting the material properties of the spacer. An average Young's modulus was determined, which is the tangent of the line connecting the origin and the connection point of the two functions describing the stress-strain relationship. The damping ratio was chosen to be 0.2, which is based on the values reported in [8].

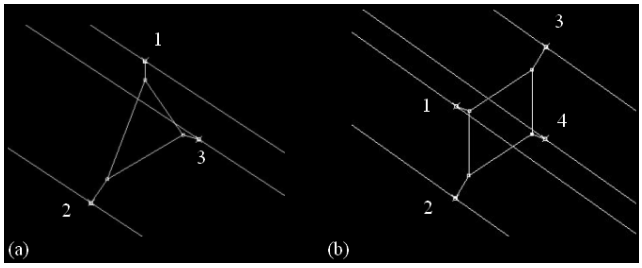

Fig. 2. Model of spacers (a) triple bundle, (b) quad bundle

IV. Results and Discussion

Five different configurations of a single span of an overhead transmission line with fixed end-points are modeled in the present study: single cable, twin bundle with spacers in the horizontal plane, twin bundle with spacers in the vertical plane, triple bundle and quad bundle. Ice sheds from one subconductor of the bundle, which is the upper cable in the triple bundle case (subconductor 1 in Fig. 2a), and one of the upper cables for the quad bundle (subconductor 1 in Fig. 2b). Ice shedding from lower cable and ice shedding from upper cable are both simulated for the twin bundle with spacers in the vertical plane. The conductors used for the simulations are Condor ACSR 54/7 and Bersfort ACSR 48/7, which are made of 54 and 48 aluminum alloy strands, respectively, reinforced with a seven-wire steel core. Cable data and parameters describing the span in static equilibrium are listed in Table I. Six load cases are examined with different ice thickness ranging from 10 mm up to 60 mm. The maximum ice thickness was chosen to correspond with the ice load considered as the extreme case under natural conditions. Table II and Table III summarize the ice loads in the different load cases, the

increased cable densities due to ice load and the coefficients of structural and aerodynamic damping for the Condor and Bersfort conductors, respectively. The number of spacers or the distance between adjacent spacers in the span under scrutiny is also varied in consecutive simulations. Since span length is constant, the application of 1, 2, 3, 4 and 5 spacers corresponds to a respective distance of 100, 67, 50, 40 and 33 m between adjacent spacers. It should be noticed that these values cover the range of 40 to 60 m which is generally used on the Hydro-Quebec transmission lines, although with unequal sub-span lengths. The reason of this fact is that spans divided into equal sub-spans are more easily subjected to oscillation, since all the sub-spans vibrate at the same time with the same horizontal frequency. In this section, we will discuss the effects of three parameters, (i) ice thickness, (ii) distance between adjacent spacers, and (iii) number of subconductors in the bundle, on the characteristics of the vibration induced by ice shedding, more precisely, on (i) the maximum jump height of the cable which ice sheds from, (ii) the maximum drop of the cable (or cables) which remain loaded, and (iii) the maximum cable tension arising during the vibration.

TABLE I
GEOMETRICAL AND MATERIAL DATA OF CABLE AND SPAN

Parameter	Unit	Condor	Bersfort
Cable diameter	(mm)	27.8	35.6
Cross-sectional area of the cable	(mm^2)	455.1	747.1
Weight per unit length of the cable	(N/m)	14.9	23.2
Cable density	(kg/m^3)	3337	3171
Young's modulus of the cable	(GPa)	68.3	67.6
Span length	(m)	200	200
Sag of unloaded cable	(m)	6	6
Initial cable tension	(kN)	12.43	19.39

TABLE II
DENSITY AND DAMPING VALUES FOR DIFFERENT ICE LOADS FOR CONDOR CONDUCTOR

Ice thickness	Ice load	Increased density of cable	Coefficient of structural damping	Coefficient of aerodynamic damping
(mm)	(N/m)	(kg/m^3)	(-)	(-)
0	0	3337	275	0.044
10	10.5	5685	1794	0.076
20	26.5	9276	2291	0.108
30	48.1	14110	2826	0.139
40	75.2	20186	3380	0.171
50	107.9	27505	3945	0.203
60	146.1	36066	4517	0.235

TABLE III
DENSITY AND DAMPING VALUES FOR DIFFERENT ICE LOADS FOR BERSFORT CONDUCTOR

Ice thickness	Ice load	Increased density of cable	Coefficient of structural damping	Coefficient of aerodynamic damping
(mm)	(N/m)	(kg/m^3)	(-)	(-)
0	0	3171	438	0.057
10	12.7	4897	2719	0.088
20	30.8	7379	3337	0.120
30	54.6	10619	4003	0.152
40	83.9	14615	4697	0.184
50	118.7	19369	5407	0.215
60	159.1	24879	6128	0.247

A. Maximum Jump Height of the Cable which Ice Sheds from

Ice thickness was varied between 10 mm and 60 mm, and the conductor bundle was connected by 3 spacers in the first set of simulations. Fig. 3a shows values of maximum jump height of the ice-shedding cable above its unloaded position, which arises during one of the first few cycles of vibration. It is clear from this figure that there is a steep increase in jump height for a single cable with increasing ice thickness, that increase being significantly slower for twin bundles, and less than 0.1 m for triple and quad bundles, for ice thickness of 30 mm and more. The results obtained for twin bundles in horizontal plane are so close to those in vertical plane that only the latter ones are presented in Fig. 3a. Likewise, due to similarity between maximum jump heights in triple and quad bundles, the figure shows only those obtained for quad bundle. If the increase in jump height is approximated by a power function of ice thickness, then the power in the best-fit function decreases from 2 to 0.1 – 0.2 as the number of subconductors is increased from 1 to 4 (see Table IV). The jump height of a single cable in the extreme case, i.e. after the shedding of 60-mm-thick ice chunk is not shown in Fig. 3a, but it was calculated as 5.84 m, and 10.25 m, for the Bersfort and the Condor conductor, respectively. Thus, the jump height of a single Condor conductor is significantly greater than that

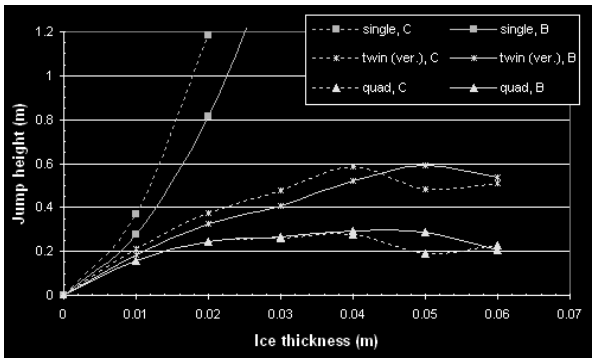

(a)

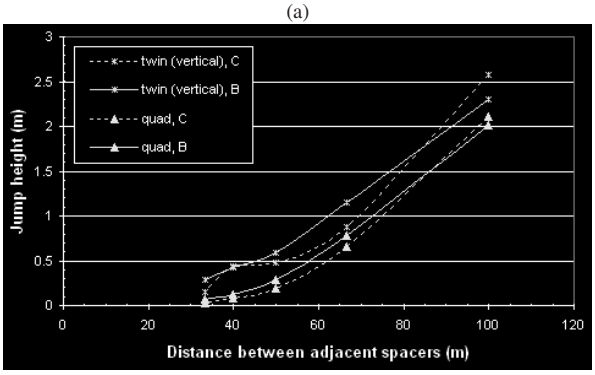

(b)

Fig. 3. Maximum jump height of the ice-shedding cable above unloaded position, C – Condor conductor, B – Bersfort conductor, (a) distance between adjacent spacers: 50 m, (b) ice thickness: 50 mm

of a Bersfort one, due to the different geometrical and material properties of these cables. However, the jump heights of bundled conductors are in the same range for the two types of conductors considered.

The number of spacers was varied between 1 and 5, while ice thickness was set to 50 mm in the next series of simulations. The increase in maximum jump height of the ice-shedding cable above its unloaded position as a function of adjacent spacer distance is shown in Fig. 3b. Jump height decreases as the number of subconductors increases. The increase in jump height with adjacent spacer distance becomes slightly steeper as the number of subconductors increases, as shown numerically by the approximate functions in Table V.

TABLE IV

PARAMETERS IN A FUNCTION OF THE FORM $y = ax^p$ APPROXIMATING MAXIMUM JUMP HEIGHT IN M, *Y*, AS A FUNCTION OF ICE THICKNESS IN M, *X*

Bundle	Condor		Bersfort	
	a	*p*	*a*	*p*
Single	2670	2.0	1580	2.0
Twin (hor.)	3.9	0.6	3.3	0.6
Twin (ver.)	2.4	0.5	3.3	0.6
Triple	0.5	0.2	0.5	0.2
Quad	0.3	0.1	0.5	0.2

TABLE V

PARAMETERS IN A FUNCTION OF THE FORM $y = ax^p$ APPROXIMATING MAXIMUM JUMP HEIGHT IN M, *Y*, AS A FUNCTION OF DISTANCE BETWEEN ADJACENT SPACERS IN M, *X*

Bundle	Condor		Bersfort	
	a	*p*	*a*	*p*
Twin (hor.)	$6.9 \cdot 10^{-5}$	2.3	$1.5 \cdot 10^{-4}$	2.1
Twin (ver.)	$2.6 \cdot 10^{-5}$	2.5	$1.5 \cdot 10^{-4}$	2.1
Triple	$9 \cdot 10^{-6}$	2.7	$1.3 \cdot 10^{-5}$	2.6
Quad	$2 \cdot 10^{-6}$	3.0	$8 \cdot 10^{-6}$	2.7

B. Maximum Drop of the Cables which Remain Loaded

The lowest position during vibration of the cable system is reached by one of the cables which remain loaded. Fig. 4a shows that the maximum drop below the unloaded position increases proportionally with ice thickness, and it is about 30-40% greater for Condor conductor than for Bersfort conductor. The curves representing the maximum drop for different bundles of the same conductor almost coincide, which can be explained by the following fact. The drop below the loaded position is significantly lower than the increase in the sag due to ice load (around 10-15%), and the increase of the sag due to ice load is approximately the same for each configuration. However, the decrease of maximum drop below the loaded position with the number of subconductors is significant. Table VI provides the coefficients and powers in the best-fit power functions approximating the maximum drop below unloaded position as a function of ice thickness.

A similar tendency may be observed in Fig. 4b, where the maximum drops below the loaded position are shown as a function of the distance between adjacent spacers. The maximum drop in absolute value decreases with the number of subconductors in the bundle. However, the difference between Figs. 3b and 4b is striking. The maximum jump height increases with the distance between adjacent spacers, while the maximum drop is significantly greater for distances of 40 and 67 m (4 and 2 spacers, respectively), than for distances of 33, 60 and 100 m (5, 3 and 1 spacer(s), respectively). This result is due to the fact that there is no spacer at mid-span when the number of spacers is even, so that the maximum drop occurs at mid-span where the cable drop can be considerably greater. It should be clear that a power function of the form $y = ax^p$ is not applicable to approximate the maximum drop below loaded position as a function of the distance between adjacent spacers. If we consider the maximum drop below the unloaded position, then its value varies by a maximum of 5% only, for an odd number of

TABLE VI

PARAMETERS IN A FUNCTION OF THE FORM $y = ax^p$ APPROXIMATING MAXIMUM DROP BELOW LOADED POSITION IN M, *Y*, AS A FUNCTION OF ICE THICKNESS IN M, *X*

Bundle	Condor		Bersfort	
	a	*p*	*a*	*p*
Twin (hor.)	-89	1.2	-50	1.1
Twin (ver.)	-89	1.2	-50	1.1
Triple	-86	1.2	-65	1.2
Quad	-85	1.2	-87	1.3

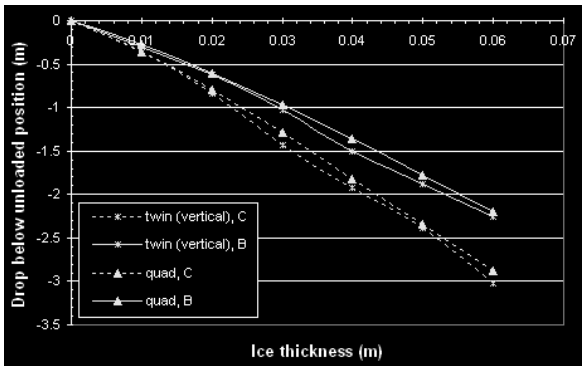

(a)

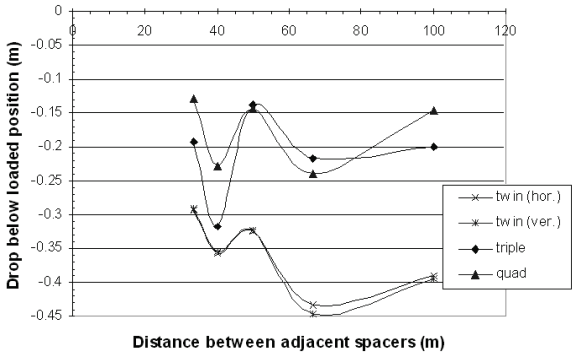

(b)

Fig. 4. Maximum drop of the cable which remains loaded (a) below unloaded position, C – Condor conductor, B – Bersfort conductor, distance between

adjacent spacers: 50 m, (b) below loaded position, Bersfort conductor, ice thickness: 50 mm

spacers, and is about 5-15% greater when the number of spacers is even.

If ice sheds from the lower subconductor while the upper one remains loaded, then the possibility of contacts between the vibrating conductors will increase as compared with the case when ice sheds from the upper subconductor (in case of a heavy ice load, they will be in contact even in static equilibrium). However, since the maximum jump and the maximum drop usually do not appear at the same location along the span, the distance between two corresponding points involving two subconductors should be calculated during vibration in order to know when the above-mentioned contact may occur. The selected points are the mid-points of the sub-spans closest to the middle of the span, because that is where the vibration is expected to have the highest amplitude. The minimum distance between these points as ice thickness and spacer distance vary are shown in Figs. 5a and 5b, respectively, in the case of a twin bundle in vertical plane. In this context, it is clear that the distances should be positive. However, negative values appear in the graphs, because they provide information as to what extent the spacing between the conductors should be increased in order to prevent contacts. According to Fig. 5a, vibrating conductors will contact if ice thickness is at least 30 mm even if the spacer distance is only 33 m. Furthermore, if this distance is increased to 100 m, impact will occur for the lowest ice loads considered, and obviously for all the other load cases which are not shown in the diagram. Fig. 5b confirms the severity of the problems arising during vibration. Only the two curves, for ice thickness

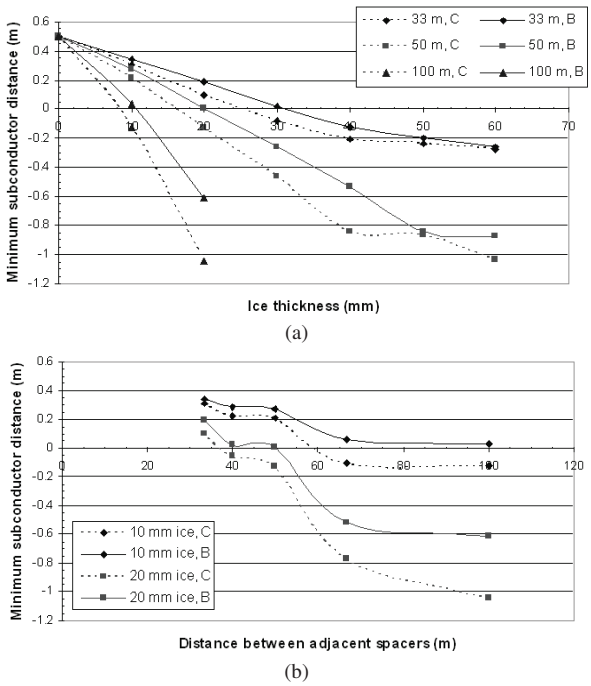

Fig. 5. Minimum distance between selected corresponding points involving two subconductors (the mid-points of the sub-spans closest to the middle of the span) during vibration (twin bundle in the vertical plane), C – Condor conductor, B – Bersfort conductor, (a) parameter is distance between adjacent spacers, (b) parameter is ice thickness

of 10 and 20 mm, are plotted in this graph. If the ice thickness is 30 mm or higher, contact occurs in all cases examined. Figs. 6a and 6b represent the minimum distance between two conductors in static equilibrium when the lower conductor is bare and the upper one is still loaded. If the spacer distance is 33 m, the conductors will not touch each other even for the highest ice load; otherwise, if the distance increases, contact may occur even in static equilibrium. Fig. 6b provides the maximum spacer distance for different ice loads when contact is avoided in static equilibrium. If the spacer distance is greater than the value given by the intersection of a curve with the horizontal line drawn at the diameter of the conductor, then conductors will touch each other. It can also be observed in Figs. 5 and 6 that the minimum subconductor distance is, in general, greater for the Bersfort conductor, i.e. the threat of contact between conductors is less severe. We must keep in mind, however, that the above discussion refers to the case when ice sheds completely from one conductor while the other one remains fully loaded. It should be noted, however, that the model may easily be adapted to simulate ice shedding from more than one subconductor, or to simulate partial shedding, by changing the material properties of some cable elements in the dynamic analysis.

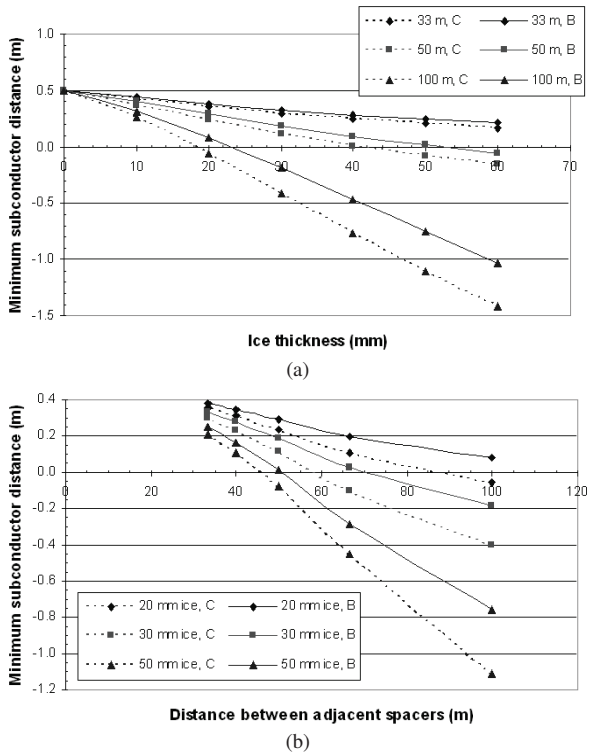

Fig. 6. Minimum distance between the two subconductors in static equilibrium when the lower conductor is bare, and the upper one is still loaded (twin bundle in the vertical plane), C – Condor conductor, B – Bersfort conductor, (a) parameter is distance between adjacent spacers, (b) parameter is ice thickness

C. Maximum Cable Tension

The calculation of cable tension is also important, since high transient dynamic forces may damage the cable or other

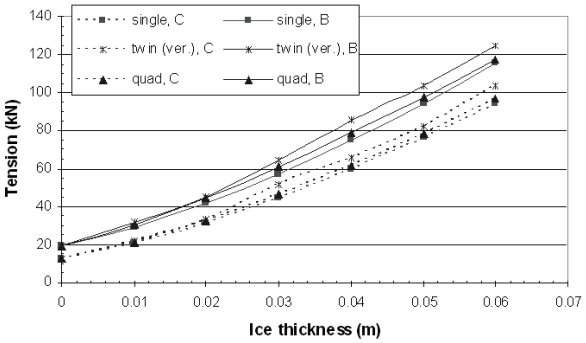

(a)

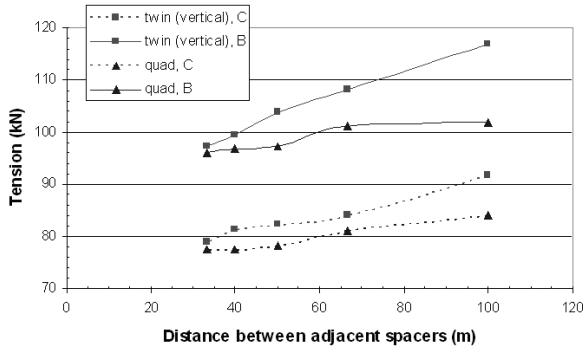

(b)

Fig. 7. Maximum cable tension, C – Condor conductor, B – Bersfort conductor, (a) distance between adjacent spacers: 50 m, (b) ice thickness: 50 mm

elements of the transmission line. The maximum tension during vibration occurs near a suspension or a spacer. Figs. 7a and 7b show the increase in cable tension as a function of shedding-ice thickness and spacer distance, respectively. Cable tension is lowest for a single cable because there are no constraints from other cables. It is highest for a twin bundle, and it decreases with the number of subconductors in the bundle. This tendency is also observed in the best-fit approximate power functions given in Tables VII and VIII. The cable tension of the Bersfort conductor is greater than that of the Condor conductor due to the former's greater weight (see Table I). The critical load at which the suspension structure fails was estimated at 100 kN in [18], although this value depends on the particular suspension structure. For the Condor conductor, this value is exceeded only after the shedding of a 60-mm ice chunk from a twin-bundled subconductor. For the Bersfort conductor, however, it is exceeded for all configurations after the shedding of a 60-mm ice chunk, and it is also exceeded in some cases after the shedding of a 50-mm ice chunk.

V. Conclusions

Vibration of bundled conductors following ice shedding from one subconductor has been the subject of this study. In particular, three parameters, thickness of ice load, distance between adjacent spacers and number of subconductors in a bundle were varied, whereas the maximum jump height of the cable which ice sheds from, the maximum drop of the cables which remain loaded and the maximum cable tension were compared for different ice-shedding scenarios. The latter variables were approximated as simple power functions of the former ones for two types of conductors. Although these power functions depend on further parameters such as span length, they were found to be useful tools to express qualitative relationship between the parameters examined. The following main conclusions are drawn from this study:

1) The displacements and the cable tension during vibration increase with ice thickness. The maximum cable tension for the highest ice loads (50 and 60 mm) may damage the suspension structure. This problem warrants further investigation because cable tension also depends on some parameters which were not varied or considered in this study such as the sag to span ratio or the flexible suspension structures.
2) The maximum jump height and the cable tension increase with the distance between adjacent spacers. The maximum drop, however, also depends on whether the number of spacers is even or odd assuming constant distance between each adjacent spacer. If the number of spacers is even, it means there is no spacer in the middle of the span, so that the maximum drop will be significantly greater than for the odd case.
3) Increasing the number of subconductors reduces the severity of vibration. Comparing twin bundles as to the horizontal and vertical plane shows that the severity of vibration is approximately the same, although the

TABLE VII

Parameters in a Function of the Form $y = ax^p + y_0$ Approximating Cable Tension in N, Y, as a Function of Ice Thickness in m, X

Bundle	Condor ($y_0 = 12430$ N)		Bersfort ($y_0 = 19390$ N)	
	a	p	a	p
Single	$3.1 \cdot 10^6$	1.3	$5.0 \cdot 10^6$	1.4
Twin (hor.)	$4.9 \cdot 10^6$	1.4	$4.2 \cdot 10^6$	1.3
Twin (ver.)	$3.5 \cdot 10^6$	1.3	$4.2 \cdot 10^6$	1.3
Triple	$3.3 \cdot 10^6$	1.3	$3.0 \cdot 10^6$	1.2
Quad	$3.3 \cdot 10^6$	1.3	$3.8 \cdot 10^6$	1.3

TABLE VIII

Parameters in a Function of the Form $y = ax^p + y_0$ Approximating Cable Tension in N, Y, as a Function of Distance between Adjacent Spacers in m, X

Bundle	Condor ($y_0 = 76200$ N)		Bersfort ($y_0 = 94190$ N)	
	a	p	a	p
Twin (hor.)	160	1.0	130	1.1
Twin (ver.)	37	1.3	130	1.1
Triple	26	1.3	43	1.2
Quad	20	1.8	52	1.1

vibration was found to be slightly more severe for the horizontal structure in case of Condor conductor. The maximum jump height of a single conductor is significantly greater than that of a conductor bundle; the cable tension, however, is slightly lower for a single conductor during vibration, since no constraint is transmitted from other cables in this case.

4) The comparison of the Bersfort and Condor conductors reveals that the maximum jump heights of ice-shedding cables in bundled conductors are in the same range. The maximum drops of cables which remain loaded as well as the jump heights of single cables are greater for the Condor conductor while the cable tension is greater for the Bersfort conductor.

In the simulations carried out in this study, ice sheds completely from one subconductor while the other ones remain fully loaded. Naturally, high-amplitude vibration may break the ice accumulated on the other subconductors and thereby induce further ice shedding. Thus, in a future development of the model, the mechanical properties of ice and ice failure during vibration could be considered. Other recommendations would be to investigate the effect of ice shedding on the torsion of the bundle and to evaluate simulation results by comparing them to experimental observations.

VI. Acknowledgment

This work was carried out within the framework of the NSERC/Hydro-Quebec/UQAC Industrial Chair on Atmospheric Icing of Power Network Equipment (CIGELE) at Université du Quebec à Chicoutimi. The authors would like to thank all the sponsors of this project, as well as Mr. P. van Dyke of Hydro-Québec for the pictures of line spacers.

VII. References

[1] V. T. Morgan, D. A. Swift, "Jump height of overhead-line conductors after the sudden release of ice loads," *Proceedings of IEE*, vol. 111, no. 10, pp. 1736-1746, 1964.

[2] A. Jamaleddine, G. McClure, J. Rousselet, R. Beauchemin, "Simulation of Ice Shedding on Electrical Transmission Lines Using ADINA," *Computers & Structures,* vol. 47, no. 4/5, pp. 523-536, 1993.

[3] M. Roshan Fekr, G. McClure, "Numerical modelling of the dynamic response of ice shedding on electrical transmission lines," *Atmospheric Research*, vol. 46, pp. 1-11, 1998.

[4] M. Roshan Fekr, G. McClure, D. Hartmann, "Investigation of Transmission Line Failure Due to Ice Shedding Using Dynamic Analysis," in *Proceedings of the 8th International Workshop on Atmospheric Icing of Structures*, Reykjavik, Iceland, 1998, pp. 11-16.

[5] L. E. Kollar, M. Farzaneh, "Dynamic Analysis of Overhead Cable Vibrations as a Result of Ice Shedding," in *Proceedings of 6th International Symposium on Cable Dynamics*, Charleston, SC, USA, 2005, pp. 427-434.

[6] T. Kalman, G. McClure, M. Farzaneh, L. E. Kollar, A. Leblond, "Dynamic Behavior of Iced Overhead Cables Subjected to Mechanical Shocks," in *Proceedings of the 6th International Symposium on Cable Dynamics*, Charleston, SC, USA, 2005, pp. 339-346.

[7] ADINA R & D, *ADINA – Theory and Modeling Guide*, Watertown, MA, USA, 2003, Report ARD 03-7.

[8] C. Hardy, P. Bourdon, "The Influence of Spacer Dynamic Properties in the Control of Bundle Conductor Motion," *IEEE Transactions on Power Apparatus and Systems*, vol. PAS-99(2), pp. 790-799, 1980.

[9] A. T. Edwards, J. M. Boyd, "Bundle-Conductor-Spacer Design Requirements and Development of "Spacer-Vibration-Damper"," *IEEE Transactions on Power Apparatus and Systems,* vol. PAS-84(10), pp. 924-932, 1965.

[10] CIGRE SCB2 WG11, "State of the Art Survey on Spacers and Spacer Dampers", Electra No. 277, August 2005.

[11] K. Anderson, P. Hagedorn, "On the Energy Dissipation in Spacer Dampers in Bundled Conductors of Overhead Transmission Lines," *Journal of Sound and Vibration*, vol. 180, no. 4, pp. 539-556, 1995.

[12] P. Hagedorn, N. Mitra, T. Hadulla, "Vortex-Excited Vibrations in Bundled Conductors: A Mathematical Model," *Journal of Fluids and Structures*, vol. 16, no. 7, pp. 843-854, 2002.

[13] C. Hardy, P. van Dyke, "Field Observations on Wind-Induced Conductor Motions," *Journal of Fluids and Structures*, vol. 9, pp. 43-60, 1995.

[14] H. M. Irvine, *Cable Structures,* MIT Press, Cambridge, MA, USA, 1981.

[15] A. B. Peabody, G. McClure, "Modeling the overhead power line post spring-damper using ADINA," in *Proceedings of the 3rd MIT Conference on Computational Fluid and Solid Mechanics*, Cambridge, MA, USA, 2005.

[16] L. E. Kollar, M. Farzaneh, "Dynamic Behavior of Cable Systems with Spacers Following Ice Shedding," in *Proceedings of ICNPAA 2006: Mathematical Problems in Engineering and Aerospace Sciences,* Budapest, Hungary, 2006.

[17] Bathe, K-J., *Finite Element Procedures*, Prentice Hall, Upper Saddle River, New Jersey, USA, 1996.

[18] M. Lapointe, "Dynamic analysis of a power line subjected to longitudinal loads," M.S. thesis, Department of Civil Engineering and Applied Mechanics, McGill University, Montreal, QC, Canada, 2003.

VIII. Biographies

László E. Kollár received a M.Sc. degree in Mechanical Engineering from the Budapest University of Technology and Economics, Hungary in 1997, a Ph.D. degree in Mechanical Engineering from the same university in 2001, and a M.Sc. degree in Mathematics from the University of Texas at Dallas, USA in 2002.

In 2002, he joined CIGELE/INGIVRE at the University of Quebec at Chicoutimi as a Postdoctoral Fellow, where he currently is a Research Professor on grant. His research interests include theoretical and experimental modeling of atmospheric icing processes and ice shedding from cables. He previously worked on the modeling of controlled unstable mechanical systems with time delay.

Masoud Farzaneh (M' 83 - SM' 91- F'07) received his electrical engineering degree from the École Polytechnique of Iran in 1973. He received successively a doctoral degree in engineering from Institut nationale polytechnique and Université Paul Sabatier, in France, and a Doctorat d'État from the latter university. From 1980 to 1982, he was Associate Professor at Université des Sciences et de la Technologie d'Oran, Algeria. He joined Université du Québec à Chicoutimi (UQAC) in 1982 as a guest professor. Following this, he became a full professor, as well as founder and Director of the Master's Degree Program in Engineering. He is currently Chairholder of the NSERC/Hydro-Quebec Industrial Chair on Atmospheric Icing (CIGELE), and Chairholder of the Canada Research Chair on Atmospheric Icing Engineering of Power Networks (INGIVRE). He is also founder of the International Research Centre on Atmospheric Icing and Engineering of Power Networks (CENGIVRE) of which he is currently Director. Prof. Farzaneh is author and co-author of more than 450 scientific publications in the domain of high voltage, outdoor insulation and atmospheric icing. He is Fellow of IEEE, Fellow of the Institution of Electrical Engineers (IEE), Fellow of the Engineering Institute of Canada (EIC), Charter Member of the International Society of Offshore and Polar Engineers (ISOPE) as well as member of the New York Academy of Sciences and the American Association for the Advancement of Sciences. He is currently Associate Editor of IEEE Transactions on Dielectrics and Electrical Insulation, Chairman of the IEEE DEIS Outdoor Insulation Committee, as

well as Chairman or member of several working groups and task forces of IEEE and CIGRÉ dealing with atmospheric icing of HV equipment.